Receptor-Mediated Binding of IgE-Sensitized Rat Basophilic Leukemia Cells to Antigen-Coated Substrates Under Hydrodynamic Flow

Linda A. Tempelman and Daniel A. Hammer
School of Chemical Engineering, Cornell University, Ithaca, New York 14853

ABSTRACT The physiological function of many cells is dependent on their ability to adhere via receptors to ligand-coated surfaces under fluid flow. We have developed a model experimental system to measure cell adhesion as a function of cell and surface chemistry and fluid flow. Using a parallel-plate flow chamber, we measured the binding of rat basophilic leukemia cells preincubated with anti-dinitrophenol IgE antibody to polyacrylamide gels covalently derivatized with 2,4-dinitrophenol. The rat basophilic leukemia cells' binding behavior is binary: cells are either adherent or continue to travel at their hydrodynamic velocity, and the transition between these two states is abrupt. The spatial location of adherent cells shows cells can adhere many cell diameters down the length of the gel, suggesting that adhesion is a probabilistic process. The majority of experiments were performed in the excess ligand limit in which adhesion depends strongly on the number of receptors but weakly on ligand density. Only 5-fold changes in IgE surface density or in shear rate were necessary to change adhesion from complete to indistinguishable from negative control. Adhesion showed a hyperbolic dependence on shear rate. By performing experiments with two IgE-antigen configurations in which the kinetic rates of receptor-ligand binding are different, we demonstrate that the forward rate of reaction of the receptor-ligand pair is more important than its thermodynamic affinity in the regulation of binding under hydrodynamic flow. In fact, adhesion increases with increasing receptor-ligand reaction rate or decreasing shear rate, and scales with a single dimensionless parameter which compares the relative rates of reaction to fluid shear.

INTRODUCTION

Receptor-mediated cell adhesion plays a crucial role in such physiological processes as the leukocyte-mediated inflammatory response, lymphocyte homing, and cancer cell metastasis. Receptor-mediated cell adhesion has also been exploited in biotechnological processes such as cell affinity chromatography (Hertz et al., 1985; Hammer et al., 1987). Many static assays, such as the centrifugation assay, have been performed to study adhesive strength, confirm putative receptor-ligand pairs and study spreading of cells (McClay et al., 1981; Schnaar et al., 1989; Chu et al., 1993). However, the dynamics of fluid flow adds an additional complexity to the study of adhesion. Most studies of the role of fluid flow on adhesion use simple shear flow in a parallel-plate or radial flow chamber. Simple shear flow is easy to generate in the laboratory, is a good model for cell/vessel wall interactions and is a start to understanding the effect of flow on adhesion in more complex hydrodynamic flows. Flow assays have been used to study attachment (Doroszewski, 1980; Lawrence et al., 1990; Wattenbarger et al., 1990; Lawrence and Springer 1991; Tissot et al., 1991; Menter et al., 1992) and detachment (Cozens-Roberts et al., 1990a, c; Kuo and Lauffenburger, 1993); we generally consider attachment and detachment to be distinct phenomena.

A rather dramatic demonstration for the need to study adhesion under flow has been provided in the neutrophil-endothelium system. In this system both P-selectin (CD62) and ICAM-1-coated surfaces support adhesion in static assays, while only P-selectin surfaces support adhesion under flow (Lawrence and Springer, 1991). Also of interest is that neutrophil binding to P-selectin results an unusual form of cell-substrate interaction called cell rolling in which cells move at a fraction of the expected hydrodynamic velocity of an unencumbered particle (Lawrence and Springer, 1991; Hammer and Apte, 1992). Studies of adhesion under flow with systems other than the neutrophil (Wattenbarger et al., 1990; Tissot et al., 1991; Mentor et al., 1992; Hammer et al., 1993) have shown that it is more common for cells to travel at their hydrodynamic velocity before sticking fairly abruptly. Dynamic simulation methods used by Hammer and Apte (1992) provide some insight into the factors which control the dynamics of adhesion, but more data for how adhesion depends on the rate of bond formation and bond micromechanics is needed to complete the picture.

A number of model systems have been developed to study the effect of cell and surface chemistry on adhesion. These approaches include liposomes (Wattenbarger et al., 1990), protein-coated hard spheres (Cozens-Roberts et al., 1990a, b; Kuo and Lauffenburger, 1993) and cellular systems in which surface chemistry has been varied (Doroszewski, 1980; Tempelman and Hammer, 1990). While noncellular model systems provide useful information about the role of chemistry in adhesion, cellular systems remain important to illustrate how model systems relate to cellular systems, and to understand how complications of cellular systems, such as deformability and surface topography, affect adhesion. Several studies (Tissot et al., 1992; Tempelman et al., 1993) have

Received for publication 26 March 1993 and in final form 7 January 1994.

Address reprint requests to Dr. Hammer. Tel.: 607-255-8681; Fax: 607-255-9166; E-mail: hammer@cheme.cornell.edu.

L. Tempelman's current address is Naval Research Laboratory, Center for Bio/Molecular Science and Engineering, Code 6900, Washington, DC 20375-5000.

0006-3495/94/04/1231/13 $2.00

observed that, in the absence of adhesive interactions, cells do not always travel at the hydrodynamic velocity predicted for a hard, smooth particle near a wall in shear flow (Goldman et al., 1967). This can significantly affect adhesion since cell velocity is a strong factor in adhesion. In addition, many cells have a microvilliated topography which affects the number of receptors available for binding with a surface.

Most previous cell attachment work has been performed in parallel-plate flow chambers. Doroszewski's early work (1980) on murine leukemia cells binding to glass at low shear rates ($\dot{\gamma} \leq 10\ s^{-1}$) used a glass substrate coated with serum proteins. Wattenbarger and colleagues (1990) measured glycophorin-coated liposomes binding to a lectin-coated surface. They were limited to a low shear rate range ($\dot{\gamma} \leq 22\ s^{-1}$), but could adjust the number of glycophorin molecules from 10^2 to 10^4 per 4 μm diameter liposome. Tissot and coworkers (1991) measured the adhesion of rat thymocytes to concanavalin A at an extremely low shear rate of $0.73\ s^{-1}$. Lawrence and Springer (1991) studied adhesion of neutrophils to P-selectin and ICAM-1 surfaces at a wide range of shear rates ($\dot{\gamma} \sim 20$–$360\ s^{-1}$) and a range of ligand densities (25–400 sites/μm^2 for P-selectin). However, their method of adjusting the number of different cellular receptors was to chemically stimulate the neutrophils. Menter and colleagues (1992) used several melanoma cell lines to measure adhesion to fibronectin or wheat-germ agglutinin under different shear rates and pharmacological treatments. To date, there has been no study of cell attachment under flow in which receptor number, ligand density, and flow rate all have been systematically varied.

In this paper we describe a model experimental system using rat basophilic leukemia (RBL) cells which allows us to carefully manipulate these variables. Adhesion is mediated by binding between cell-bound IgE and surface antigen; the Fc portion of IgE is bound to RBL cell surface Fc_ϵ receptors. Many characteristics of the cell, such as the number of its Fc_ϵ receptors ($1–3 \times 10^5$ (Metzger et al., 1986)) are known. We selected the RBL cell system both because of morphological similarities to leukocytes (Oliver et al., 1986) and because a battery of well-characterized reagents, such as antigen-IgE pairs of known affinity and kinetics, have been developed for this system in the course of its use as a model system for studying the relationship between receptor cross-linking and secretion (Metzger et al., 1986; Erickson et al., 1987). In this study, we use a single antigen, dinitrophenol (DNP) and an anti-DNP IgE antibody. The number of anti-DNP IgE surface molecules, and hence the binding sites for DNP, is changed by adjusting the ratio of anti-DNP IgE to another IgE (directed against a neutral antigen) which is used to fill the remaining Fc_ϵ receptors (Fig. 1 *A*). Measured in solution, the affinity between the antibody and DNP is $K_A = 10^8\ M^{-1}$ and the forward rate constant is $k_f = 10^7\ M^{-1}\ s^{-1}$ (Erickson et al., 1987). With this single IgE-antigen system, an alternate binding avenue exists by prebinding the antibody bivalently to the gel and using the recognition between the Fc_ϵ receptor and the Fc portion of IgE to mediate adhesion (Fig. 1 *B*). The affinity for Fc binding to the Fc_ϵ receptor is 100-fold higher ($10^{10}\ M^{-1}$) but the forward rate constant is only $10^5\ M^{-1}\ s^{-1}$ (Metzger et al., 1986). An additional advantage is that the RBL cells can be grown in culture and large numbers of relatively homogenous cells can be easily obtained.

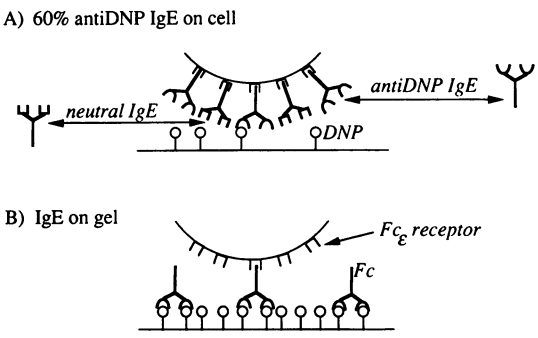

FIGURE 1 Control of number of binding sites and binding kinetics. (*A*) High k_f system used predominantly in these experiments. RBL cells are preincubated with a mixture of excess antibody. The relative proportion of anti-DNP IgE and another nonreactive IgE controls the number of binding sites for DNP. In this paper, 0, 20, 60, or 100% of the 2×10^5 Fc_ϵ receptors were filled with anti-DNP IgE. (*B*) Low k_f system. Antibodies are bivalently bound to a highly derivatized DNP gel and cells adhere to the antibody-coated surface via a Fc to Fc_ϵ receptor bond. The second system has a 100-fold higher affinity, but a 100-fold lower forward reaction rate as measured in solution than the system in *A*.

We use a bifunctional linker to covalently attach 2,4-DNP-ϵ-lysine by its free primary amine group by an amide linkage to a thin polyacrylamide gel. This technology was previously developed by Schnaar and colleagues for the attachment of amino sugars, peptides, and proteins to gels for adhesion studies (Schnaar and Lee, 1975; Pless et al., 1983). The DNP-coated gel has a number of attractive features for adhesion. It is translucent, so we can view cells through it using an inverted microscope. Bare gels (without antigen) support almost no nonspecific adhesion of cells (Chu et al., 1994). Since DNP is covalently linked to the gel, DNP is unlikely to be removed by flow or by cells.

We use a parallel-plate flow chamber (Fig. 2) to measure the adhesion of RBL cells to the DNP-coated surface over a wide range of shear rates ($\sim$20–150 s^{-1}). The chamber contains a thin polyacrylamide gel that has been derivatized on the downstream half with DNP. RBL cells coated with anti-DNP IgE do not bind to portions of the gel without DNP. Therefore, we can allow the cells to settle on the non-DNP portion of the gel, initiate the flow through the chamber and measure the binding dynamics as the cells move onto the DNP portion of the gel.

In this study, we used our experimental system to elucidate the effects of shear rate, receptor density, and ligand density on cell attachment. We also changed the kinetics of receptor-ligand bond formation by preincubating the antibody with the substrate, which gives a reduced forward rate of reaction despite a higher affinity. The results show that a decrease in the kinetics of bond formation leads to a decrease in cell adhesion under flow, but that adhesion can be recovered by

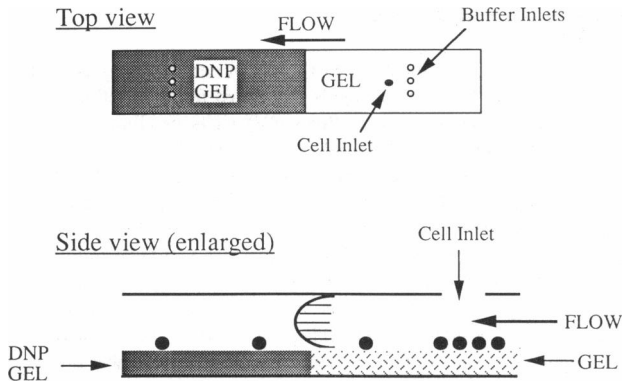

FIGURE 2 Parallel-plate flow chamber. The gel is divided into two portions: a non-DNP region where cells settle at the start of the experiment and a DNP portion onto which cells flow and have an opportunity to bind during the experiment. Cells are not depicted to scale; the true cell diameter is 1/40 of the chamber height.

incubating the cells with the substrate for sufficiently long to allow bond formation. We believe this is the first study in which receptor number, ligand density, and shear stress have been simultaneously varied in attachment experiments involving real cells, as well as the first experiments which directly correlate kinetics of bond formation with the extent of cell attachment.

MATERIALS AND METHODS

Antibody-coated cells

The RBL subline 2H3 (Barsumian et al., 1981) was a gift from Dr. C. M. S. Fewtrell. These cells were cultured and harvested as described by Taurog and coworkers (Taurog et al., 1979) for use between days 4 and 7. RBL cells are spherical, and our subline measured a 13-μm diameter (Model ZM Coulter Counter, Hileah, FL, and brightfield microscopy) and are highly microvilliated with 3000 microvilli (based on transmission electron microscopy (Oliver et al., 1988)). Microvilli are 0.5 μm long (Oliver et al. 1988) with a cross sectional area of 0.01 μm^2 (Oliver et al., 1988; Bongrand and Bell, 1984). RBL cells possess on average 2×10^5 $Fc_\epsilon R1$ receptors (Metzger et al., 1986; Ryan, 1989).

Purified mouse monoclonal anti-2,4-dinitrophenol IgE from hybridoma H1 26.82 (Lui et al., 1980) was a generous gift from Drs. B. Baird and D. Holowka. Mouse monoclonal anti-dansyl IgE from clone 2774 (PharMingen, San Diego, CA) was used as a neutral antibody that does not bind DNP. Cells (2×10^6/ml) were incubated in a 24 nM antibody mixture for at least 30 min. The anti-DNP to anti-dansyl ratio was adjusted to fill between 0 and 100% of the RBL cell's $Fc_\epsilon R1$ receptors with anti-DNP IgE (Weetal, 1992). In this way, we change the number of binding sites for DNP from 0, 20, 60, or 100% of 4×10^5 (IgE is bivalent). The cells were centrifuged and resuspended in a modified Tyrodes buffer (125 mM NaCl, 5 mM KCl, 10 mM 4-(2-hydroxyethyl)-1-piperazineethanesulfonic acid (HEPES), 1 mM $MgCl_2$, 1.8 mM $CaCl_2$, 0.05% gelatin, and 5.6 mM glucose in deionized water) at 3–4 $\times 10^5$ cells/ml and held at 37°C under gentle agitation in a waterbath for use within several hours. Control experiments and one experiment (described later in the text) were done without adding antibody.

Antigen-coated gels

Gel preparation

Acrylamide, *N,N'*-methylene-bis-acrylamide, *N,N,N',N'*-tetramethylethylene diamine (TMED), and ammonium persulfate were from Bio-Rad Laboratories (Hercules, CA). High percent acrylamide (21 g of monomer/100 ml) gels which were also highly cross-linked (0.083 g of cross-linker/(g cross-linker + monomer)) were cast using 0.25-μm Teflon spacers in a vertical gel caster (SE215 or 275 Hoeffer Scientific, San Francisco, CA). The solution was buffered with 54 mM HEPES to pH 6.0. 162 μl of TMED and 429 μl of 7% w/v ammonium persulfate per 100 ml were used as initializers. The monomer solution contained 1.25–20 mM of the *N*-succinimidyl ester of acrylamidohexanoic acid, a bifunctional linker, which copolymerizes with acrylamide. The linker was synthesized in our laboratory using the method of Pless and coworkers (Pless et al., 1983). Dr. B. Brandley (Glycomed, Alameda CA) provided us with advice on the chemistry of linker synthesis and a sample of linker to use as a crystallization seed.

Derivatization

After casting for 1 h and rinsing gels in cold water for 15 min, half the gel is inactivated by reacting the linker with ethanolamine at 1 μl/ml in 50 mM HEPES in deionized water with 10% ethanol buffer (pH 8.0) for 5 min. This step is performed by dipping the gel vertically in this capping solution and rinsing thoroughly with water. The entire gel is then treated horizontally with a saturated solution (5.3 mM) of *N*-ϵ-2,4-DNP-lysine hydrochloride (Sigma, St. Louis MO) in 50 mM HEPES with 10% ethanol buffer (pH 8.0) for 60–150 min. The DNP attaches to the active half of the gel by an amide linkage, displacing *N*-hydroxysuccinimide. A final 30-min treatment with ethanolamine solution caps any unreacted linker sites with a methyl group, preventing the formation of charged carboxyl groups that would result from further hydrolysis of the linker. Reaction parameters were chosen to maximize aminolysis (attachment of DNP) and minimize hydrolysis (Schnaar and Lee, 1975; Pless et al., 1983). Normally, the amount of DNP in a gel is controlled by the amount of linker in the gel and varies linearly with linker concentration (Chu et al., 1993). However, for one experiment described in the text, two short timed dips (1 and 5 min) of a 20-μmol linker/ml gel provided a single gel with two parallel regions with different levels of derivatization.

DNP surface density

Circles of gel were cut (1.45-cm diameter, 0.025-cm height), covered with 5 N NaOH and incubated at 37°C for 16–17 h. This liberated the DNP from the gel, and the solution was assayed for DNP spectrophotometrically at 365 nm (Milton Roy Spectronic 1001 plus). The assay was calibrated with known concentrations of DNP-lysine HCl which had also been treated with 5 N NaOH. The results gave the efficiency of the derivatization reaction to be approximately 0.5 μmol of DNP/μmol linker. The volumetric density was converted to a surface density using the assumption that DNP molecules within the top 10 Å of the gel would be accessible to antibody bound to cells moving across the surface. The surface density of DNP for gels with 1.25 μmol of linker/ml of gel, which were used in the majority of our experiments, is approximately 3.6×10^{10} molecules/cm^2.

Several saturation binding experiments of ^{125}I-anti-DNP IgE to DNP gels were performed to assess levels of DNP or IgE bound to the gels. These experiments did not give an absolute DNP surface concentration, because, in the time necessary for equilibrium binding between IgE and gel-bound DNP, the IgE in solution was able to penetrate beyond the surface of the gel. The level of IgE association with the gel far exceeded the density of linker in the gel's upper surface, suggesting deep (>100 Å) penetration of the IgE into the gel. Thus, saturation binding overestimates the density of DNP available to cell-bound antibody. However, a saturation binding study on a 1.25 μmol/ml gel gave the same level of binding as a subsaturation binding (23.9 nM) to a 20 μmol/ml gel. Also, the characteristic time for dissociation of half the IgE bound at subsaturation on the 20 μmol/ml gel was over 3 h, indicating that antibody was bivalently bound to the gel. Details can be found in Tempelman (1993). This information is used to compare ligand density in experiments presented later in the text.

Ratio of receptor and ligand densities

For many microvilliated leukocyte cells, there is a two- to threefold excess surface area (Evans and Yeung, 1989). Based on our measurement of cell radius and microvilli number and size, the total RBL cell area, A, is $A = 4\pi R_c^2 + N_{mv}\pi L_{mv}D_{mv}$, where R_c is cell radius, N_{mv} is microvilli number, L_{mv} is microvilli length, and D_{mv} is microvilli diameter. Therefore, $A = 4\pi(6\ \mu m)^2 + 3000\pi(0.1\ \mu m)(0.5\ \mu m) = 923\ \mu m^2$. Comparison to the projected area, $4\pi R_c^2$, shows this is a twofold excess area. Therefore, the average cell surface receptor density is (number of $Fc_\epsilon R1$ receptors/area = $2 \times 10^5/923\ \mu m^2 =$) 217 $Fc_\epsilon R1/\mu m^2$. This is two receptors per microvillus tip (tip area 0.01 μm^2). Since only receptors at the tips of microvilli area available for binding, the effective number of receptors is (217 $Fc_\epsilon R1/mm^2$)-(3000 microvilli)(0.01 μm^2/microvilli) = 6.5×10^3 $Fc_\epsilon R1$, or 12.2 receptors/mm^2. Using this number and estimates of DNP density on the gel, we can compare ligand and receptor densities to determine which are in excess. For example, on a 1.25-μmol linker/ml gel with 100% anti-DNP IgE the ratio of surface ligand to cell binding sites would be:

$$\frac{\text{Ligand density}}{\text{Cell binding site density}} = \frac{3.5 \times 10^{10}(\text{DNP/cm}^2)}{[2(\text{Binding sites/IgE})][1.2 \times 10^9(\text{Fc}_\epsilon \text{ receptors/cm}^2)]} = 15$$

For combinations of anti-DNP IgE and DNP surface density used in our experiments, the ligand/anti-DNP IgE ratio is given in Table 1. Note that for all conditions of interest, binding is limited by the density of cell binding sites rather than the density of ligand.

Flow chamber and equipment

The flow chamber is a parallel-plate chamber with a separate inlet for cells and accommodations to hold a thin gel. The channel for fluid flow has dimensions of $72 \times 15.2 \times 0.53$ μm (L × W × H). A simplified schematic drawing of the flow channel is shown in Fig. 2; additional details are available in Tempelman (1993). In brief, the chamber is made from two blocks of transparent Lexan which are held together with plastic screws. The bottom piece has a double width microscope slide for visualization which is secured into the chamber with silicon glue. The slide is recessed from the chamber bottom to accommodate the gel. The top piece has the buffer inlet and outlet ports as well as the separate cell inlet port. The height of the channel is determined by a Silastic™ Sheeting gasket (Dow Corning, Midland MI) which is 0.021 inches thick. Buffer flow to the chamber is provided by a syringe pump (Sage Model 355, Orion Research Incorp., Boston MA) using a 500-ml glass syringe (Scientific Glass Engineering, Austin TX) and volumetric flow rates were measured daily and compared to a pump calibration curve. Cells are observed under 200 × magnification on an inverted stage microscope (Nikon Diaphot-TMD) using phase contrast optics. The experiments are videorecorded (Dage-MTI 67S Newvicon videocamera; JVC BR-S611 videoplayer) for analysis at a later time. A thermal printer (Sony VideoGraphic Printer UP-870 MD) was used to make prints of some videoframes.

TABLE 1 Ratio of DNP (ligand) to IgE (receptor) densities

Linker concentration (μmol linker/ml)	% anti-DNP IgE	Ligand Density / Receptor density
0.74	20	44
0.74	100	9
1.25	20	73
1.25	100	15
10.0	20	1300
10.0	100	250

Adhesion experiment

The chamber is filled with modified Tyrodes buffer. In the absence of buffer flow, 20–40 μl of cell suspension is introduced from the cell inlet using a 500-μl syringe (Hamilton Corp., Reno, NV). Cells are allowed to settle for approximately 4 min onto the non-DNP portion of the gel. The inlet region is scanned spatially and videotaped in a systematic manner. The 20 × microscope objective is then positioned downstream along the centerline of the chamber just within the adhesive region of the gel. Buffer flow is directed into the chamber for a period of time more than sufficient for all cells to travel the length of the chamber. Then the DNP region of the gel is scanned systematically. Negligible numbers of cells remain adherent to the region of the gel near the cell inlet despite being on the surface under static conditions for a significant length of time. Between trials, the flow chamber is cleared of cells by the high shear force of purging the chamber with water and air. Then a duplicate trial is performed. Analysis of duplicate and triplicate trials shows gel adhesiveness is not affected by repeated use of the gel.

Analysis

Three-dimensional plots of the cell inlet region and the DNP region are prepared using WingZ™ (Informax Software, Lenexa, KS) software. The fraction of adhesion is calculated as the total number of cells adhered in the DNP region divided by the number of cells initially observed in the inlet region. Only individual cells are counted in the inlet and in the DNP region; doublets, triplets, and clumps are ignored. Our method of cell delivery ensures that the vast majority of cells are at the bottom of the chamber. This makes a comparison of the number of cells that attach to the DNP portion of the gel with the number of cells counted in the inlet area a particularly meaningful measure. If cells were present at all separation distances in the inlet fluid (as cells have been in previous researchers' adhesion systems), visualization of cells interacting with the substrate and determination of the number of cells available for binding would be more complicated and ambiguous.

Error in cell counting

While a counting error in any individual field of view may be ±5%, the errors are random and the total error over about 300 fields was measured to be only 1%. Error in scanning the gel systematically is about 5%. This is because scanning is done rather quickly both to speed the experiment and also to minimize the time bound cells remain on the gel. This can lead to as much as a ±10% error (calculated) in percent adhesion which is only 1% error for 10% adhesion, but 10% error for 100% adhesion.

Methods of determining shear rate

For most trials, wall shear rate is calculated based on the measured volumetric flow rate and channel dimensions, $\dot{\gamma} = Q/40Wd^2$, where $\dot{\gamma}$ is the wall shear rate in s^{-1}, Q is the volumetric flow rate in milliliters/min, W is the chamber width in centimeters, and d is the channel half height in centimeters. Wall shear stress is proportional to wall shear rate; the proportionality factor is the viscosity, which we have measured to be 0.0106 g/cm-s for modified Tyrodes buffer (Tempelman, 1993).

Clearly, flow rate is not a unique indicator of shear rate, since, in day-to-day assembly of the chamber, the height $2d$ may vary. Therefore, for some trials, we further confirmed shear rate by measuring the population average velocity of cells traveling across a 650-μm field of view (at the beginning of the DNP region of the gel), and comparing it to the average velocity for 14.5-μm diameter polystyrene beads (Coulter Corp., Hialeah, FL) (Tempelman, 1993). Because the dependence of bead velocity on shear rate agreed fairly well with theory (Goldman et al., 1967), calibration curves could be constructed which related bead velocity to shear rate, and hence cell velocity to shear rate. This technique was used for an extensive study of RBL cell motion in simple shear (Tempelman et al., 1994); interested readers are directed there for further information.

RESULTS

Control experiments

To test for nonspecific adhesion under flow, we measured the adhesion of RBL cells without antibody to DNP-coated gels. Duplicate runs at 22 s^{-1} showed less than 3% adhesion (21 bound out of 2014 and 124 out of 4373). A control at a higher shear rate of 99 s^{-1} gave 0 out of 1804 cells bound. This control and others (cells with anti-dansyl IgE on DNP gels, cells with and without antibody on non-DNP gels) also showed low nonspecific adhesion in a static assay (Chu et al., 1994).

Location of binding

At high DNP concentrations (>10 μmol linker/ml), it is possible to see the DNP portion of the gel, because DNP absorbs in the yellow (as well as in the UV). We have observed that cells adhere only on the DNP region of the gel. At lower DNP concentrations the yellow demarcation cannot be clearly seen, but the start of cell adhesion remains distinct and can be used to mark (infer) the border of the DNP region. In Fig. 3, we show a series of videoprints which map the interface between DNP-free and DNP-derivatized portions of the gel after an adhesion experiment; here, the DNP density in the derivatized portion of the gel was 3.6×10^{10} molecules/cm^2. Although there is an occasional cell adhering slightly before the DNP-free/DNP-derivatized interface or well inside the non-DNP portion, there is well-defined separation between regions of the gel which support adhesion (DNP-derivatized) and regions which do not (DNP-free).

Bimodal binding behavior

Fig. 4 demonstrates several important dynamic features of adhesion in this experimental system. A field of view was selected which spanned the boundary between a DNP and non-DNP region of the gel. The number of frames (1/30 s) for individual cells to travel the first 223 μm (non-DNP region) and last 223 μm (DNP region) of the 650-μm field were recorded for 57 cells. The average velocities in the non-DNP and DNP portions of the gel were 1.4 and 1.5 cm/min, respectively. (We consistently observed that RBL cells moved more quickly over the DNP portion of the gel, which we attribute at least in part to unknown nonspecific interactions which modulated RBL cell-substrate separation distance). The data demonstrate that cells coated with anti-DNP IgE do not travel at a reduced velocity over a DNP-coated surface before they bind. In fact, over the entire range of experimental conditions tested, there was no indication that RBL cells make transient bonds which reduce their velocity without leading to complete adhesion. We observed that cells move with a constant velocity right up until the last few frames (<0.1 s) before coming to a stop. Most cells stopped quite abruptly, but occasionally a cell would pause, turn over once, and then stop. Fig. 4 also demonstrates that there is a spread in cellular velocities due to some inhomogeneity in the size or shape of cells and perhaps in their separation distance from the surface.

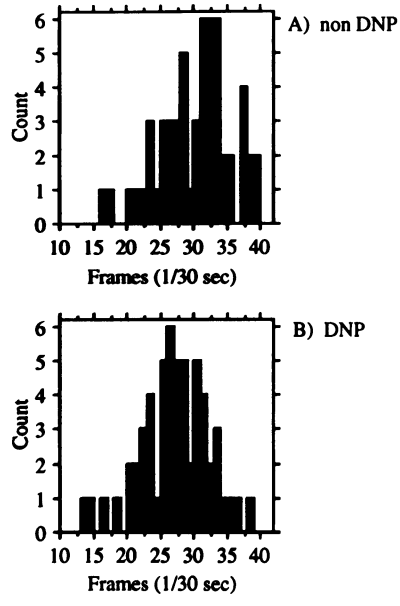

FIGURE 4 The number of frames (1/30 s) it takes cells coated with 20% anti-DNP IgE to travel across 223 μm of gel. The averages are 30 (SD = 5) and 27 (SD = 5) frames for travel over non-DNP (*A*) and DNP (*B*) portions of gel, respectively. This corresponds to velocities of 1.4 and 1.5 cm/min. This shows that RBL cells do not travel at a reduced velocity on a DNP-coated surface prior to firm adhesion.

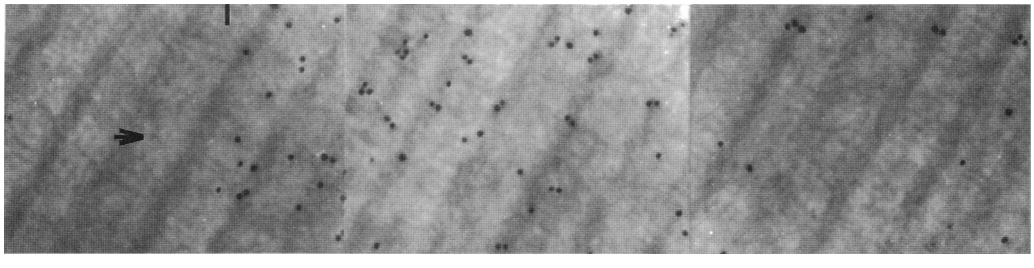

FIGURE 3 Videoprint of adhesion of RBL cells treated with anti-DNP IgE on DNP-coated gel. This series shows a 0.48 × 2 μm (L × W) portion of the channel spanning the interface between non-DNP and DNP portions of the gel. The demarcation between non-DNP and DNP sections of the gels is indicated by a line, and the arrow shows the direction of flow. Here 100% of the $Fc_\epsilon R$ were filled with anti-DNP IgE, the gel contained 3.6×10^{10} molecules DNP/cm^2 gel and $\dot{\gamma}$ was 65 s^{-1}.

Effect of shear rate

Fig. 5 *A* shows cell adhesion as a function of shear rate for two levels of anti-DNP IgE at a fixed ligand density of 3.6×10^{10} molecules/cm^2. For 20% anti-DNP IgE, adhesion is complete at about $\dot{\gamma} = 20\ s^{-1}$ and becomes becomes quite sparse at $\dot{\gamma} \geq 100\ s^{-1}$. Two days' experiments with individual data points are shown. For 100% anti-DNP IgE, complete adhesion is supported at $\dot{\gamma} \leq 70\ s^{-1}$, but adhesion drops off rapidly to less than 10% adhesion at $\dot{\gamma} = 99\ s^{-1}$. 60% anti-DNP IgE data is not shown, because it is similar to the 100% anti-DNP data as will be obvious in Fig. 7. Fig. 5 *B* shows the linear relationship between adhesion and inverse shear rate for the 20% anti-DNP IgE experiments of Fig. 5 *A*.

The spatial patterns of adhesion for experiments at three different shear rates from the 20% anti-DNP IgE curve of Fig. 5 *A* are shown in Fig. 6. Total adhesion decreases as shear rate increases, and the spatial pattern appears to change with shear rate. At the lowest shear rate ($\dot{\gamma} = 26\ s^{-1}$) where adhesion is 75%, there is a high density of adherent cells at the start of the DNP region, and the density of adherent cells decreases with distance down the chamber. At higher shear rates the pattern of binding appears disperse, almost independent of position. Binding continues greater than 1500 cell diameters from the beginning of the DNP-gel and might continue further if the flow chamber were longer. This shows there is a small, nonzero probability of adhesion at all positions down the length of the chamber.

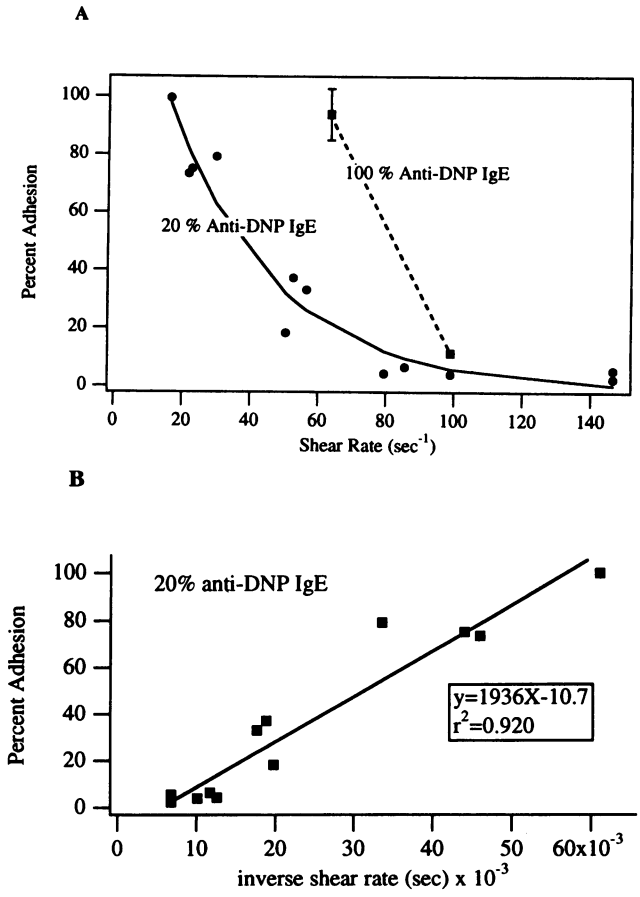

FIGURE 5 (*A*) Total adhesion as a function of shear rate for two levels of receptors. For a fixed ligand density (3.6×10^{10} molecules/cm^2) and 20% anti-DNP IgE, the percentage of the cells added to the chamber which adhered decreased sharply as shear rate was increased. Data for individual trials is shown and shear rate was calculated from average cell velocity. For 100% anti-DNP IgE, the curve is shifted to higher shear and falls off even more steeply. Average adhesion with standard error is shown for simplicity. (*B*) Percent adhesion replotted as a function of inverse shear rate for 20% anti-DNP IgE.

Effect of receptor number

Total percent adhesion is also affected by the number of binding sites on the cell. Fig. 7 shows adhesion for 20, 60, and 100% anti-DNP IgE on the cells for three shear rates at a fixed ligand density of 3.6×10^{10} molecules/cm^2. For the lowest shear rate ($\dot{\gamma} = 30\ s^{-1}$) adhesion is already very high when there is only 20% anti-DNP IgE, and we assume higher levels of anti-DNP IgE would also lead to nearly complete adhesion. For the highest shear rate ($\dot{\gamma} = 99\ s^{-1}$), the maximum level of adhesion is 11%, even at the highest anti-DNP IgE surface density. At the middle shear rate, $\dot{\gamma} = 64\ s^{-1}$, we see the most sensitivity to anti-DNP IgE surface density. When the number of binding sites is increased from 20 to 60% anti-DNP IgE (a threefold increase) the amount of adhesion increases from an average of 23% to 100% (a 4.4-fold increase).

Three-dimensional plots of adhesion at $\dot{\gamma} = 64\ s^{-1}$ are shown in Fig. 8. Both 60% anti-DNP IgE and 100% anti-DNP IgE show distinct ridges of adhesion where the DNP portion of the gel begins and show similar amounts of total adhesion. The 20% anti-DNP IgE trial shows a flatter, more diffuse pattern of adhesion.

Effect of ligand density

A special gel was prepared so that adhesion on two different ligand densities could be measured simultaneously in a single experiment. Parallel sections of a 20-μmol linker/ml gel were derivatized for either 1 or 5 min leading to DNP densities which differed 14-fold when measured by the DNP base hydrolysis method (see Materials and Methods). Adhesion was tested at two levels of receptor density and two shear rates. Although there is some increase in adhesion on the higher ligand density gels, there is a more significant increase in adhesion as shear rate is decreased or as percent anti-DNP IgE is increased (Fig. 9). The weak dependence on ligand density, but strong dependence on anti-DNP IgE surface density, is expected since the ligand density is in excess compared to the receptor density (see Materials and Methods and Table 1).

Effect of bond kinetics

Fig. 10 *A* shows the percent adhesion at various shear rates for two different surface chemistries which are known to exhibit different binding kinetics. The "high k_f" system is

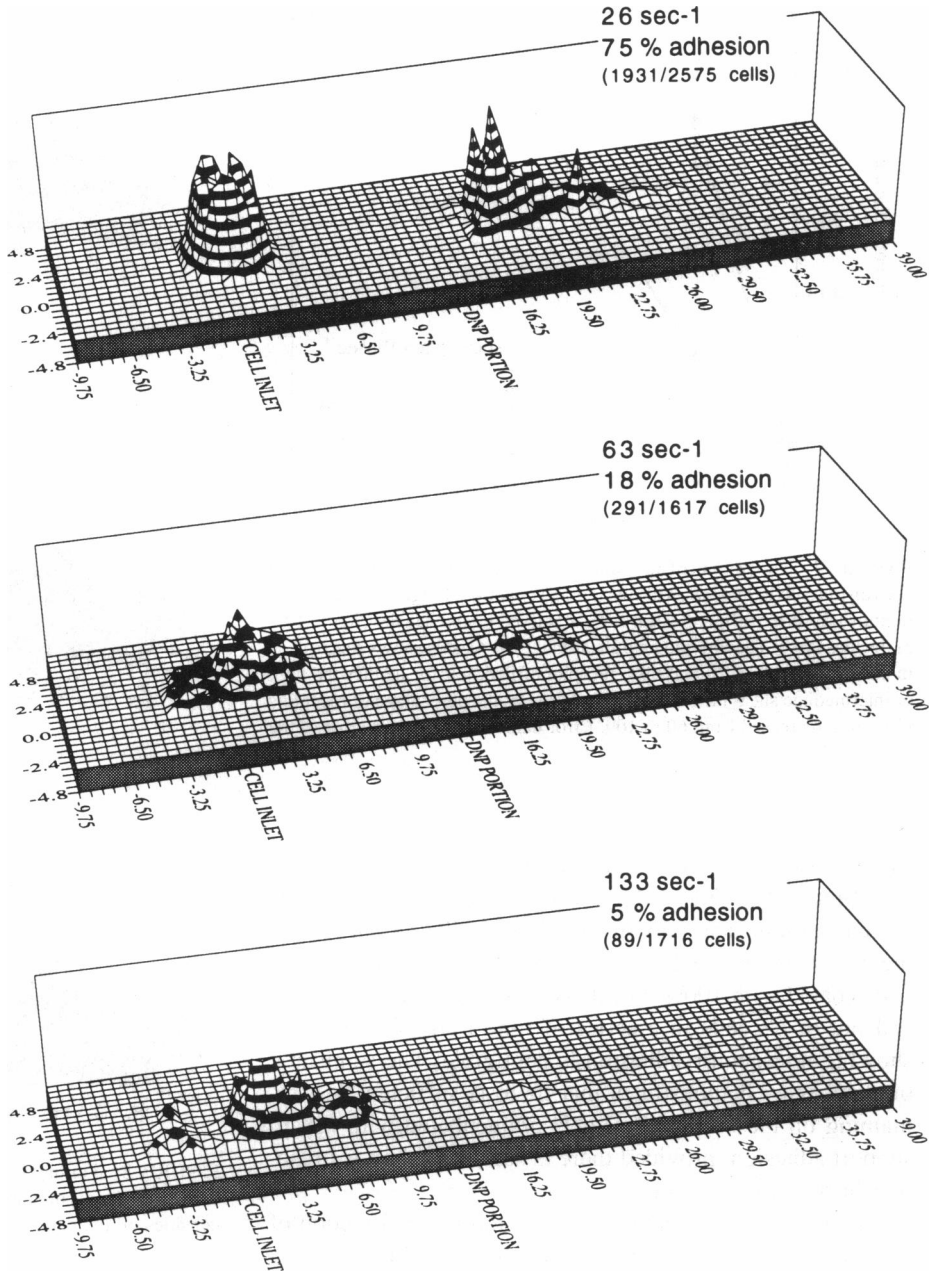

FIGURE 6 Spatial patterns of adhesion as a function of shear rate. These three-dimensional plots show the number of cells in each 650 × 480 μm field before (*left*) and after (*right*) each experiment. At the lowest of the three shear rates, there is clearly a large amount of adhesion (seen as a "ridge") at the start of the DNP portion with adhesion tapering off with distance down the chamber. Adhesion continues to occur >1500 cell diameters downstream in some trials. Distances are in millimeters. Striations represent units of six cells.

where a mixture of anti-DNP and anti-dansyl IgE is preincubated with the cells. As we previously noted, the high k_f system displays a kinetic rate of binding of $k_f = 10^7\ M^{-1}\ s^{-1}$ (Erickson et al., 1987). This is the binding system used to generate the data presented in Figs. 3–9. The "low k_f" system is where anti-DNP IgE was preincubated on high density DNP (20 μmol linker/ml) gels at 23.9 nM, and the cells were free of antibody as shown in Fig. 1 *B*. The low k_f system displays a kinetic rate of recognition of $k_f = 10^5\ M^{-1}\ s^{-1}$ (Metzger et al., 1986). Adhesion is very low for the low k_f system. For example, the high k_f system at 99 s^{-1} can support more adhesion on average than the low k_f system at 30 s^{-1}. Differences between high k_f and low k_f systems are not due to differences in ligand density; the density of surface binding sites is similar for both systems (see Materials and Methods). That is, the number of DNP sites on a 1.25-μmol linker/ml gel (3.6×10^{10} molecules/cm^2) is similar to the number of Fc ends available on a 20-μmol linker/ml gel after a 2 h incubation at 23.9 nM as measured by ^{125}I anti-DNP IgE binding studies (Tempelman, 1993).

Fig. 10 *B* shows a semistatic binding assay that further elucidates the differences in binding behavior between the high k_f and low k_f systems. In this assay, flow is turned on to deliver the cells to the DNP portion of the gel. Flow is turned off for the specified amount of time and then turned on to a low shear rate of 26 s^{-1} to wash away unattached cells. Percent adhesion is based on about 10 cells in this assay, and most trials were performed in quadruplet. After a 1-min incubation the difference between the two systems is striking. In the low k_f system an average of only 12% of cells bind

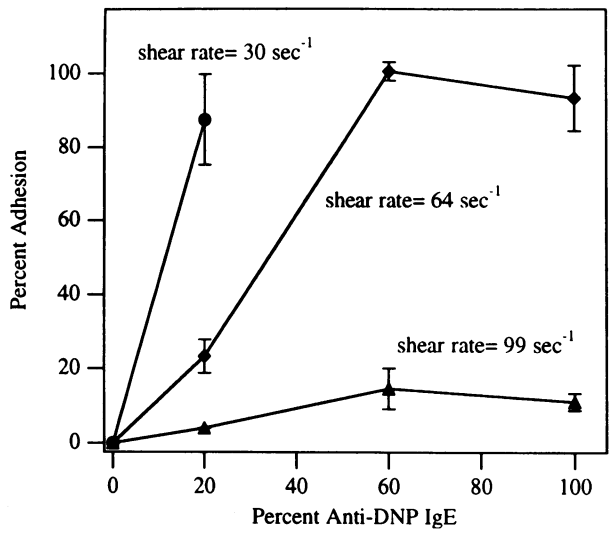

FIGURE 7 The amount of adhesion as a function of the amount of binding sites on the cell (expressed as the percentage of anti-DNP IgE in the antibody mixture) for three different shear rates at a fixed ligand density (3.6×10^{10} molecules/cm^2). The intermediate shear rate ($\dot{\gamma} = 64\ s^{-1}$) shows a sharp rise in adhesion between 20 and 60% receptors filled, but for neither the high or intermediate shear rates was an effect seen as the percentage of receptors filled was increased from 60 to 100. Error bars are ± standard error of the mean.

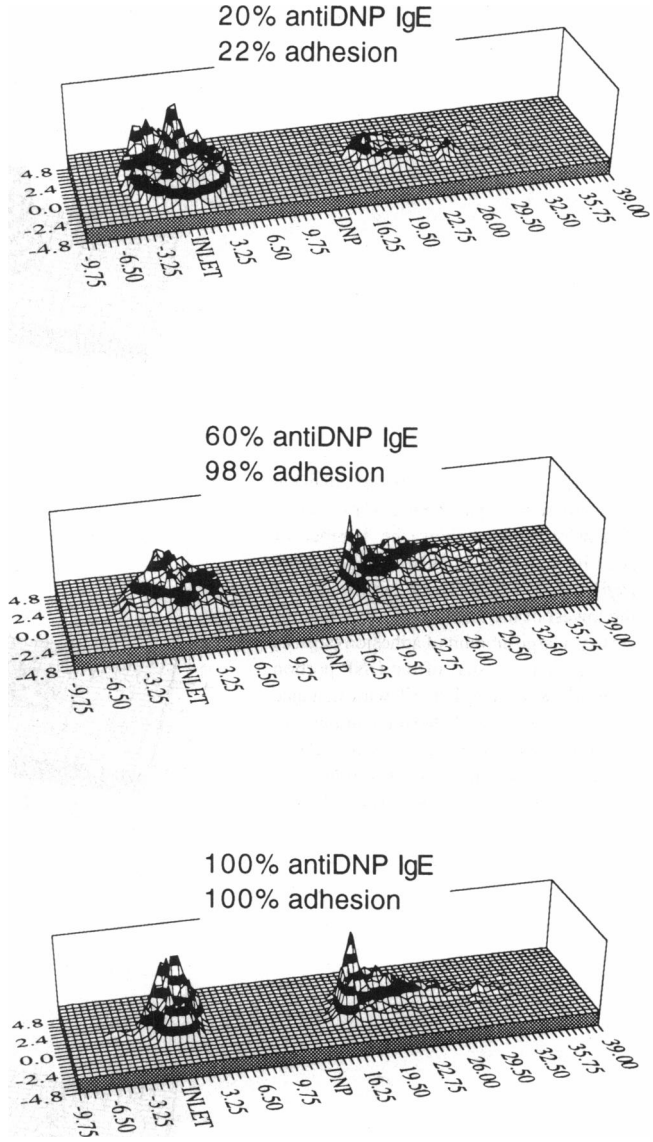

FIGURE 8 For the intermediate shear rate given in Fig. 7 (64 s^{-1}), three-dimensional plots of individual binding experiments are shown for three IgE densities on the cells.

(range, 0–30%), whereas in the high k_f system an average of 74% bind (range, 50–89%). However, after 5 min the low k_f system exhibits near maximal binding similar to that seen in the high k_f system at 1–2 min. As a control, the adhesion of cells coated with 100% anti-dansyl IgE was used. Only one cell out of 68 cells in a series of time trials bound, again showing nonspecific adhesion is negligible. The semistatic binding assay demonstrates that there is sufficient IgE remaining on the 20 μmol/ml gels preincubated with IgE to support adhesion, provided there is sufficient time for reaction in the low k_f system.

Finally, the spatial pattern of adhesion in the direction of flow is shown in a two-dimensional form in Fig. 11 for a number of different experimental conditions. Individual three-dimensional spatial plots (as shown in Figs. 6 and 8) are integrated over the chamber width and are normalized to a level of 2000 inlet cells (adherent cells/number of inlet cells × 2000). Also, trials were adjusted so that adhesion started at the same axial position, since from day to day the location of non-DNP/DNP demarcation can vary by several millimeters. The highest adhesion trial shown (high k_f, 60 s^{-1}, 100% anti-DNP IgE, 100% adhesion) has a substantial peak of bound cells; the next two trials (high k_f, 60 s^{-1} and low k_f, 99 s^{-1}) show a mild peak and show similar levels of adhesion; and the last trial (low k_f, 60 s^{-1}) has a very low, scattered pattern of adhesion. Clearly, attachment can be modulated by changes in shear rate or intrinsic bond kinetics, and in the Discussion we consider whether there might be a unifying way of scaling these two parameters.

DISCUSSION

In this paper we report results for adhesion experiments with a model cellular system, RBL cells, binding to antigen- or antibody-coated gels in a parallel-plate flow chamber. This is the first study of cell attachment in which cell surface site density, substrate ligand density, shear rate, and bond formation kinetics have all been altered. The results confirm that our gross qualitative picture of adhesion is correct. For example, adhesion increases with increasing IgE or DNP surface density, with decreasing flow rate, or with increasing bond formation kinetics.

Bimodal surface interactions

We find the interaction of RBL cells with DNP gels is bimodal: cells either continue at their hydrodynamic velocity

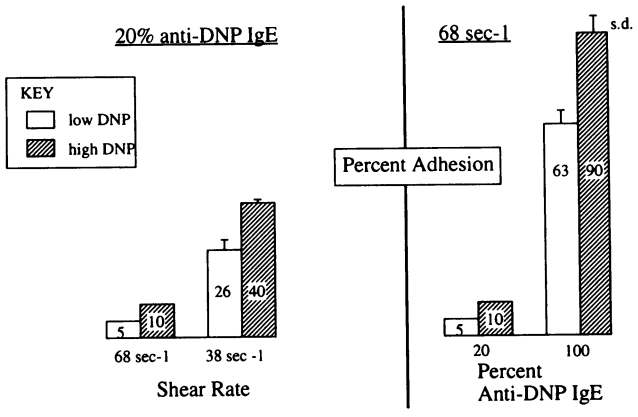

FIGURE 9 Effect of ligand density on extent of adhesion. A special gel was prepared so that adhesion on two different ligand densities could be studied side by side simultaneously. Portions of a 20-μmol linker/ml gel were derivatized for 1 or 5 min leading to DNP densities which differed 14-fold. The low density side had 0.37 and the high density side 5.0 μmol of DNP/ml gel. Adhesion was tested at two surface anti-DNP IgE concentrations and shear rates.

or are adherent. This bimodal surface interaction has also been seen by a number of different groups. Menter and coworkers (1992) measured the shear rate at which several melanoma cell lines adhered to fibronectin. They observed a sudden arrest of cells which appears similar to the dynamics of adhesion seen with RBL cells. Wattenbarger and colleagues (1990) measured the adhesion of glycophorin liposomes to lectin surfaces and reported a variety of binding behavior from abrupt permanent attachment to repeated sticking and releasing with or without final adhesion. They defined a sticking probability as the inverse of the number of adhesive contacts made by a liposome before permanent adhesion. At $\dot{\gamma} = 10$ or 22 s^{-1} for three levels of receptors, they saw an increase in sticking probability with increasing receptor number. Because they were also in a receptor-limited regime, they also saw little effect on adhesion with changing ligand density. They concluded that flow rate, particle diameter, and receptor density controlled adhesion in their model system.

Tissot and coworkers' (1990) study of rat thymocytes concentrated to a large extent on particle motion. They showed that thymocytes do not roll at a reduced velocity on concanavalin A, as we have shown here for the RBL system for a much wider range of conditions. Thymocytes also stopped abruptly and adhered. Even at an extremely low shear rate ($\dot{\gamma} = 0.73$ s^{-1}), only 24% of cells judged to be close to the surface adhered. Aldehyde-fixed cells showed decreased adhesion (14%). We do not find this surprising since fixation can alter protein conformation and availability. For example, the Fc_ϵ receptors of RBL cells are unable to bind IgE when glutaraldehyde-fixed, but do bind IgE when paraformaldehyde-fixed (Oliver et al., 1988).

Neutrophil adhesion appears to display special dynamic behavior unlike that seen in our RBL cell system. On P-selectin surfaces neutrophils roll at a reduced velocity over a wide range of shear rates, but on ICAM-1 alone the cells neither roll nor adhere. Interestingly, cells rolling on P-selectin and ICAM-1 adhere firmly upon stimulation (Lawrence and Springer, 1991).

At the time this work was initiated, no model or theory of the kinetic and biomechanical properties of receptor-ligand

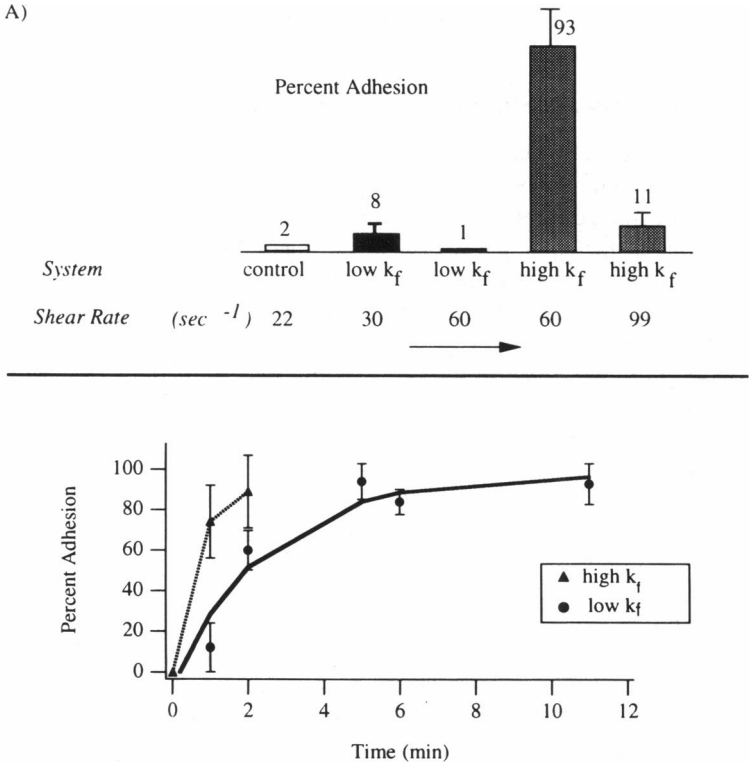

FIGURE 10 Adhesion as a function of bond kinetics. An experiment was performed where the antibody was prebound to the gel rather than to the cell (as described in the text and Fig. 1 *B*). (*A*) Adhesion is low for the low k_f system in flow experiments. (*B*) In an assay where cells are allowed to bind in the absence of flow, both the high k_f and low k_f systems lead to significant binding, but there is a longer time for binding required in the low k_f system as expected. All error bars are standard deviation.

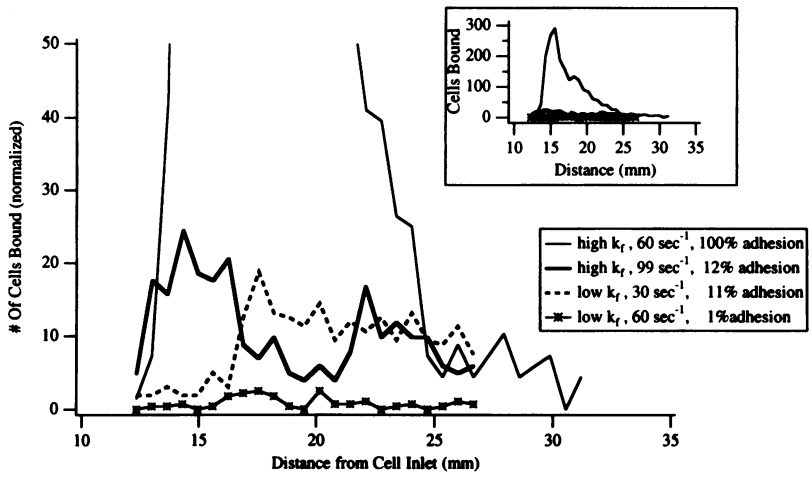

FIGURE 11 Comparison of two-dimensional spatial patterns for adhesion with different bond kinetics and shear rates. Individual three-dimensional spatial plots (of the form given in Figs. 6 and 8) are integrated over the chamber width and are normalized to a level of 2000 inlet cells (adherent cells/number of inlet cells × 2000). Adhesion increases with increasing forward reaction rate or decreasing shear rate.

bonds could predict whether a cell (or other particle) in a hydrodynamic flow would bind abruptly (Wattenbarger et al., 1990; Tissot et al., 1991; Mentor et al., 1992; Hammer et al., 1993) or roll (Lawrence et al., 1990; Lawrence and Springer, 1991). What is unique about the neutrophil system is still a subject of investigation. Hammer and Apte (1992) suggest that the bonds between neutrophils and endothelial cells may have unique rates of breakage under strain that allow bonds to be made and broken at precisely the correct rate to lead to rolling. Unfortunately, the biomechanical properties (such as a spring constant for binding or bond breakage under strain) and kinetic rates of bond formation have not been measured for enough systems to either confirm this prediction or to predict when cells *will not* roll. Our investigation provides an example of a nonrolling, bimodal system where the bond kinetics are known, although the mechanical properties of the molecules are not.

Effect of shear rate and ligand density

We observed that binding depends strongly on shear rate and on receptor number but weakly on ligand density (Fig. 9). We have considered whether the technique used to derivatize two portions of the same gel with different ligand densities actually results in the 14-fold difference in DNP surface concentration we deduce from DNP hydrolysis. It is possible the difference in DNP density we measure by volumetric density (base hydrolysis assay) represents a difference in depth of reaction rather than extent of surface derivatization. However, we have evidence that refutes this possibility. In separate studies of the time course of DNP reaction on 1.25- and 20-μmol linker/ml gels, for the 20-μmol linker/ml only 43% derivatization occurs (normalized to final derivatization) after 5 min but for the 1.25-μmol linker/ml gel, 70% derivatization occurs after 5 min. The 20-μmol linker/ml shows 70% derivatization at 10 min (Tempelman, 1993). This implies that the extent of derivatization depends on duration of reaction rather than on rate of penetration since both gels were of the same thickness. Since the DNP molecule is quite small, it seems logical that diffusion into the gel would be rapid. Thus, our best estimate is that there was indeed a 14-fold difference in DNP density.

Our explanation of why ligand density had little effect on extent of adhesion in Fig. 9 is that the ligand densities (0.37 and 5.0 μmol DNP/ml), are in excess over receptor number by at least 9- and 250-fold (Table 1). Thus, the system is receptor-limited; any receptor that finds itself in proximity to the surface finds a good supply of ligand. It would be difficult to test the system in the ligand-limited regime owing to the difficulty in producing gels with ligand densities one to two orders of magnitude lower than that currently used.

Extent of adhesion is greatly dependent on shear rate. In Fig. 5 *A* for 20% anti-DNP IgE there is a decrease in adhesion as shear rate increases; the dependence appears hyperbolic. When adhesion with 20% anti-DNP IgE data is replotted against inverse shear rate, the result is a straight line with a linear correlation coefficient of $r^2 = 0.959$ (Fig. 5 *B*). The lack of a high value of r^2 seems to be due to scatter in the data, rather than suggestion of another shape to the curve. This is logical since the total time a cell spends on the gel (and hence the time available for binding) is proportional to the inverse shear rate. At higher cell binding site densities (60 and 100% anti-DNP IgE) the range of shear rates over which binding changes from complete to negligible is too narrow to collect data at enough shear rates to determine a curve more detailed than a simple line.

Effect of receptor number

The number of binding sites on the cell has an effect only for a small range of shear rates (see Fig. 7). Below a certain threshold shear rate, any of the binding site numbers used in this study would lead to complete adhesion. Conversely, above a certain threshold shear rate, even completely decorated, 100% anti-DNP IgE cells show low adhesion. In our system the complete binding threshold is estimated to be slightly less than 30 s^{-1}, and the low binding threshold is around 99 s^{-1}. At a shear rate of 64 s^{-1}, a threefold increase in receptors (20% anti-DNP IgE to 60% anti-DNP IgE) leads to a substantial increase in binding. The presence of more

receptors obviously increases the probability that a bond will form. We were surprised by the narrow region of parameter space in which we could change receptor number and shear rate to modulate adhesion.

Analysis of rate constants

Existing theories for attachment under hydrodynamic flow suggest attachment should scale with a dimensionless forward reaction rate, $\kappa = k_f N_l/\dot{\gamma}$ (Hammer and Lauffenburger, 1987; Hammer and Apte, 1992), where N_l is the ligand density (molecules/area). κ compares the rate of reaction to the rate of hydrodynamic flow. Since k_f and $\dot{\gamma}$ were varied independently in the data shown in Fig. 11, we can test whether adhesion scales with κ.

We start with the analysis of Bell (1978), where the overall forward reaction rate is given $k_f = k_+ k_{+1}/(k_{+1} + k_-)$, where k_+ and k_- represent the rates of encounter and disengagement of the receptor-ligand pair, and include only transport effects. k_{+1} and k_{-1} denote the intrinsic forward and reverse reaction rates of the pair, respectively. k_{-1} is implicitly involved in the above expression for k_f, since the expression is only true when $k_{+1}/k_{-1} \gg 1$, a condition often obeyed by high affinity biological reactions. This expression is true for any type of transport, such as diffusion, convection, or combinations thereof. We apply this theory to understand differences between the high k_f and low k_f binding systems.

The forward rates of reaction as measured in solution for these systems are $k_f = 10^7\ M^{-1}\ s^{-1}$ for DNP-IgE (Erickson et al., 1987), and $k_f = 10^5\ M^{-1}\ s^{-1}$ for IgE-Fc$_\epsilon$R (Metzger et al., 1986). We can extract the intrinsic rate constant from the measured three-dimensional rate of reaction (Berg and Purcell, 1978; DeLisi, 1980; Shoup and Szabo, 1982) using a solution translational diffusion constant of 10^{-5} cm^2/s and obtain $k_{+1} = 4.1 \times 10^6\ s^{-1}$ for DNP-IgE, and $k_{+1} = 4.1 \times 10^4\ s^{-1}$ for IgE-Fc$_\epsilon$R. Therefore, a 100-fold difference in measured k_f in solution gives rise to a 100-fold difference in the intrinsic reaction rate, k_{+1}.

In constructing the two-dimensional overall forward reaction rate, we need to calculate the collision and dissociation of potential reactants via existing transport mechanisms. k_f can be written

$$k_f = k_+ \frac{k_{+1}}{k_{+1} + k_-} = k_+ \phi \qquad (1)$$

where k_+ and k_- are now diffusion controlled rates of transport of receptor towards and away from ligand, respectively. Bell has shown that for two-dimensional diffusive collisions, $k_+ = 2\pi D$ and $k_- = 2D/s^2$, where D is the long-time lateral self diffusion constant for the Fc receptor (2×10^{-10} cm^2/s (Menon et al., 1986)), and s is the radius of the encounter complex where receptor and ligand are close enough to react (10^{-7} cm (Bell, 1978)). ϕ is a dimensionless group which is one if the reaction is diffusion limited ($k_{+1} > k_-$), and less than one if the reaction is transport limited ($k_{+1} < k_-$). We find $\phi = 1$ for the high k_f case, and $\phi = 1/2$ for the low k_f case.

Using Eq. 1, the dimensionless parameter, k, is given

$$\kappa = \frac{k_f N_l}{\dot{\gamma}} = \frac{k_+ N_l \phi}{\dot{\gamma}} \qquad (2)$$

To compare the four k_f trials in Fig. 11, we note that surface ligand density (N_l) and k_+ are similar in all cases, but the valence for reaction, ν, is twice as high when IgE is on the cell (high k_f) than when it is on the substrate (low k_f). Therefore, we can define a new constant which isolates all the differences between the two systems, $\hat{\kappa}$, as

$$\hat{\kappa} = \frac{\kappa}{k_+ N_l} = \frac{\nu\phi}{\dot{\gamma}} \qquad (3)$$

$\hat{\kappa}$ has units of time. Note, at 60 s^{-1}, there is a 4-fold difference in $\hat{\kappa}$ between high k_f and low k_f systems. In Table 2, we compare levels of adhesion in the four experiments of Fig. 11 with values of $\hat{\kappa}$. There is very good agreement. For example, increases in adhesion are accompanied by increases in $\hat{\kappa}$. Also, two experiments, one with the high k_f and the other with the low k_f system, in which the levels of adhesion are the same, display similar values of $\hat{\kappa}$.

Several additional comments regarding this comparison are in order. First, the functional form given by Eq. 3 is also supported by Fig. 5, in which we measured that adhesion has a hyperbolic dependence on shear rate. Second, our prediction of a 4-fold difference in k_f between high k_f and low k_f systems corresponds to data in Fig. 10 *B*, in which a 4-fold longer incubation is required in the low k_f system to attain the same level of adhesion as in the high k_f system. Third, we have assumed diffusion controls transport in this system, but we have not considered the role of convection due to the slip velocity between cell and substrate surfaces, which is predicted by the hydrodynamic theory for hard sphere motion near a substrate in simple shear flow (Goldman et al., 1967). The Peclet number, Pe, can be used to judge whether convection might be important, where $Pe = V_s s/D$, and V_s is the slip velocity between cell and substrate. The slip velocity is $V_s = f\dot{\gamma} R_c$, where f is a hydrodynamic correction factor (Goldman et al., 1967). V_s is typically about half the translational velocity; at $\dot{\gamma} = 30\ s^{-1}$, $V_s = 0.5$ cm/min (Goldman et al., 1967). Therefore, $Pe = 4$ at $\dot{\gamma} = 30\ s^{-1}$, which suggests convection and diffusion have equal roles in transport. This means k_+ and k_- should be recalculated based on a theory which includes convection in the overall rate of encounter of a mobile tracer to immobile obstacles, but no such theory exists at the moment. The successful comparison between theory and experiment in Table 2 suggests that transport is still diffusion dominated, either because diffusion dominates at $Pe = 4$, or because $Pe < 4$ due to errors in predicting the

TABLE 2 Scaled forward reaction parameters

Case	$\dot{\gamma}$ (s^{-1})	F_{adh}	ϕ	$\hat{\kappa} = \nu\phi/\dot{\gamma}$ (s)
High k_f	60	1.00	1	3.3×10^{-2} ($\nu = 2$)
High k_f	99	0.12	1	2.0×10^{-2} ($\nu = 2$)
Low k_f	30	0.11	0.5	1.7×10^{-2} ($\nu = 1$)
Low k_f	60	0.01	0.5	8.3×10^{-3} ($\nu = 1$)

slip velocity from hard sphere theory. Finally, there is insufficient precision in our measurements to take this comparison further, due to experimental errors in measurement of the ligand density and to uncertainty regarding steric effects which might influence either the reaction between DNP and IgE when IgE is on the cell surface (high k_f) or the reaction between $Fc_\epsilon R$ and IgE when IgE is on the substrate (low k_f). Because only 4-fold differences in reaction rate appear to have enormous effects on adhesion, measurements of increased precision are necessary to verify the role of receptor transport in cell adhesion.

Nevertheless, it is clear the low k_f system displays lower adhesion at the same shear rate than the high k_f system, despite the low k_f system's higher affinity. Most adhesion molecules are characterized by their affinity for mutual interaction. This is in part due to ease of measurement of affinity, compared to the difficulty of measuring kinetic constants. We show here, experimentally, that attachment under flow is controlled by the forward rate of the reaction, and is independent of affinity. Of course, affinity, which might be a partial indicator of bond strength (Bell, 1978; Kuo and Lauffenburger, 1993), may determine how many bonds are necessary to hold the cell. However, if the forward rate of reaction is too slow to allow any bonds to form, the strength of the bonds is a moot point. In simulations of neutrophil rolling (Hammer and Apte, 1992) it was also found that the forward rate of reaction is a strong modulator of adhesion under hydrodynamic flow and that the affinity itself does not uniquely determine adhesion.

Spatial patterns of adhesion

In this paper we have only shown a few key examples of the three- and two-dimensional patterns of adhesion. Simulation or theoretical recreation of these spatial patterns of adhesion will provide further insight into adhesion; to guide such investigations, we provide interpretive insights into these patterns.

First, cells can adhere 20 mm, or about 1500 cell diameters, from the start of the DNP region. This indicates that cell binding is a probabilistic process (Hammer and Apte 1992; Cozens-Roberts et al., 1990c) and in this case should be modeled as such.

Second, there is often a peak in binding that occurs at the start of the DNP portion of the gel. It is not likely that a higher ligand density at the DNP/non-DNP interface is the cause; it is more likely that the DNP density is reduced there as some linker sites may have been capped. Another consideration is the effect of cell density (crowding) on adhesion. The peak in adhesion is seen when both high or low cell densities are used; therefore, cell-cell interactions do not seem to be responsible for the peak in adhesion. We have also transformed the adhesion data to account for the higher density of free cells available at the start of the DNP region and find that the percentage of adhering cells is still highest in this region. Heterogeneity in the cell population may contribute to the peak in adhesion. Both cell velocity (as seen in Fig. 4) and receptor number vary throughout the population (Ryan, 1989). Therefore, we suspect some combination of population heterogeneity and individual cell probabilistic behavior controls the observed patterns of adhesion, but distinguishing the relative importance of these two effects will require substantial calculation.

In summary, we have used a model cell system for cell attachment to ligand-coated substrates under flow. The cells, anti-DNP IgE-sensitized RBL cells binding to DNP-coated gels, display bimodal adhesion. We have varied shear rate, receptor number, ligand density, and bond formation kinetics and saw expected trends in adhesion. Importantly, this is the first study in which all these parameters have been varied in a study of cellular attachment in hydrodynamic flow.

We wish to express our appreciation to Dr. Barbara Baird and Dr. Dave Holowka for providing antibodies against DNP as well as for suggestions on choice of antibody/antigen pairs. We also thank Dr. Clare Fewtrell and Ms. Pat Cleveland for the donation of the RBL cell line. Assistance from Dr. B. A. Brandley (Glycomed, Alameda, CA) with polyacrylamide gel technology is greatly appreciated. A portion of the videotape analysis was completed by Samuel Park and Min Soo Kim.

This work was supported by the National Science Foundation in the forms of a Research Initiation Award (EET-8808867) and a Presidential Young Investigator Award (BCS-8958632) to D. A. Hammer. A Cornell Biotechnology Program Predoctoral Fellowship funded by Army Research Office supported L. Tempelman during much of this work.

REFERENCES

Barsumian, E. L., E. Isersky, M. G. Petrino, and R. P. Siraganian. 1981. IgE-induced histamine release from rat basophilic leukemia cell lines: Isolation of releasing and non-releasing clones. *Eur. J. Immunol.* 11: 317–323.

Bell, G. I. 1978. Models for the specific adhesion of cells to cells. *Science (Wash. DC).* 200:618–627.

Berg, H. C., and E. M. Purcell. 1977. Physics of chemoreception. *Biophys. J.* 20:193–219.

Bongrand, P., and G. I. Bell. 1984. Cell-cell adhesion: parameters and possible mechanisms. *In* Cell Surface Dynamics: Concepts and Models. A. S. Perelson, C. DeLisi, and F. W. Wiegel, editors. Marcel Dekker, Inc. 459–493.

Chu, L., L. A. Tempelman, C. Miller, and D. A. Hammer. 1994. Centrifugation assay of IgE-mediated rat basophilic leukemia cell adhesion to antigen-coated polyacrylamide gels. *A. I. Ch. E. J.* In press.

Cozens-Roberts, C., J. A. Quinn, and D. A. Lauffenburger. 1990a. Receptor-mediated adhesion phenomena: model studies with the radial-flow detachment assay. *Biophys. J.* 58:107–125.

Cozens-Roberts, C., D. A. Lauffenburger, and J. A. Quinn. 1990b. Receptor-mediated cell attachment and detachment kinetics: Part I—Probabilistic model and analysis. *Biophys. J.* 58:841–856.

Cozens-Roberts, C., J. A. Quinn, and D. A. Lauffenburger. 1990c. Receptor-mediated cell attachment and detachment kinetics: Part II—Experimental model studies with the radial-flow detachment assay. *Biophys. J.* 58: 857–872.

DeLisi, C. 1980. The biophysics of ligand-receptor interactions. *Quart. Rev. Biophys.* 13:201–230.

Doroszewski, J. 1980. Short-term and incomplete cell-substrate adhesion. *In* Cell Adhesion and Motility. A. S. G. Curtis, and J. D. Pitts, editors. Cambridge University Press, UK. 171–197.

Erickson, J., B. Goldstein, D. Holowka, and B. Baird. 1987. The effect of receptor density on the forward rate constant for binding of ligands to cell surface receptors. *Biophys. J.* 52:657–662.

Evans, E. A., and A. Yeung. 1989. Apparent viscosity and cortical tension of blood granulocytes determined by micropipet aspiration. *Biophys J.* 56:151–160.

Goldman, A. J., R. G. Cox, and H. Brenner. 1967. Slow viscous motion of a sphere parallel to a plane wall. II. Couette flow. *Chem. Eng. Sci.* 22: 653–660.

Hammer, D. A. 1991. Simulation of cell rolling and adhesion on surfaces in shear flow. *Cell Biophysics.* 18:145–182.

Hammer, D. A., and S. M. Apte. 1992. Simulation of cell rolling and adhesion on surfaces in shear flow: general results and analysis of selectin-mediated neutrophil adhesion. *Biophys. J.* 62:35–57.

Hammer, D. A., and D. A. Lauffenburger. 1987. A dynamical model for receptor-mediated cell adhesion to surfaces. *Biophys J.* 52:475–487

Hammer, D. A., J. J. Linderman, D. J. Graves, and D. A. Lauffenburger. 1987. Affinity chromatography for cell separations: Mathematical model and experimental analysis. *Biotech. Prog.* 3:189–204.

Hammer, D. A., L. A. Tempelman, and S. M. Apte. 1993. Statistics of cell adhesion under hydrodynamic flow: simulation and experiment. *Blood Cells.* 19:261–277.

Hertz, C. M., D. J. Graves, D. A. Lauffenburger, and F. T. Serota. 1985. Use of cell affinity chromatography for separation of lymphocyte subpopulations. *Biotech. Bioeng.* 27:603–612.

Kuo, S. C., and D. A. Lauffenburger. 1993. Relationship between receptor/ligand binding affinity and adhesion strength. *Biophys. J.* 65:In press.

Lawrence, M. B., C. W. Smith, S. G. Eskin, and L. V. McIntire. 1990. Effect of venous shear stress on CD18-mediated neutrophil adhesion to cultured endothelium. *Blood.* 75:227–237.

Lawrence, M. B., and T. A. Springer. 1991. Leukocytes roll on a selectin at physiological flow rates: distinction from and prerequisite for adhesion through integrins. *Cell.* 65:859–873.

Lui, F. T., J. W. Bohn, E. L. Ferry, H. Yamamoto, C. A. Molinaro, N. R. Klinman, and D. H. Katz. 1980. Monoclonal dinitrophenyl-specific murine IgE antibody: preparation, isolation, and characterization. *J. Immunol.* 124:2728–2736.

McClay, D. R., G. M. Wessel, and R. B. Marchase. 1981. Intercellular recognition: quantitation of initial binding events. *Proc. Natl. Acad. Sci. USA.* 78:4975–4979.

Menon, A. K., D. Holowka, W. W. Webb, and B. Baird. 1986. Clustering, mobility and triggering activity of small oligomers of immunoglobulin E on rat basophilic leukemia cells. *J. Biol. Chem.* 102:534–540.

Menter, D. G., J. T. Patton, T. V. Updyke, R. S. Kerbel, M. Maamer, L. V. McIntire, and G. L. Nicolson. 1992. Transglutaminase stabilizes melanoma adhesion under laminar flow. *Cell Biophys.* 18:123–143.

Metzger, H., G. Alcaraz, R. Hohman, J.-P. Kinet, V. Pribluda, and R. Quarto. 1986. The receptor with high affinity for immunoglobulin E. *Ann. Rev. Immunol.* 4:419–470.

Oliver, J. M., J.-C. Seagrave, R. F. Stump, J. R. Pfeiffer, and G. G. Deanin. 1988. Signal transduction and cellular response in RBL-2H3 mast cells. *Prog. Allergy.* 42:185–245.

Pless, D. D., Y.-C. Lee, S. Roseman, and R. L. Schnaar. 1983. Specific cell adhesion to immobilized glycoproteins demonstrated using new reagents for protein and glycoprotein immobilization. *J. Biol. Chem.* 258: 2340–2349.

Ryan, T. A. 1989. Signal transduction of immunoglobulin E receptor crosslinking. Ph.D. thesis. Cornell University, Ithaca, NY. 149 pp.

Schnaar, R. L., B. K. Brandley, L. K. Needham, P. Swank-Hill, and C. C. Blackburn. 1989. Adhesion of eukaryotic cells to immobilized carbohydrates. *Methods. Enzymol.* 179:542–558.

Schnaar, R. L., and Y.-C. Lee. 1975. Polyacrylamide gels copolymerized with active esters. A new medium for affinity systems. *Biochemistry.* 14:1535–1541.

Shoup, D., and A. Szabo. 1982. Role of diffusion in ligand binding to macromolecules and cell-bound receptors. *Biophys. J.* 40:33–39.

Taurog, J. D., C. Fewtrell, and E. Becker. 1979. IgE mediated triggering of rat basophilic leukemia cells: lack of evidence for serine esterase activation. *J. Immunol.* 122:2150–2153.

Tempelman, L. A. 1993. Quantifying receptor-mediated cell adhesion under hydrodynamic flow using a model cell line. Ph.D. thesis. Cornell University, Ithaca, NY. 313 pp.

Tempelman, L. A., and D. A. Hammer. 1990. Quantitating receptor-mediated cell adhesion under flow using a model cell line. *J. Cell Biol.* 111:404a.

Tissot, O., C. Foa, C. Capo, H. Brailly, M. Delaage, and P. Bongrand. 1991. Influence of adhesive bonds and surface rugosity on the interaction between rat thymocytes and flat surfaces under laminar shear flow. *J. Dispersion Sci. Technol.* 12:145–160.

Tissot, O., A. Pierres, C. Foa, M. Delaage, and P. Bongrand. 1992. Motion of cells sedimenting on a solid surface in a laminar shear flow. *Biophys J.* 61:204–215.

Wattenbarger, M. R., D. J. Graves, and D. A. Lauffenburger. 1990. Specific adhesion of glycophorin liposomes to a lectin surface in shear flow. *Biophys. J.* 57:765–777.

Weetal, M. 1992. Studies on the high affinity receptor for IgE ($Fc_\epsilon RI$): Binding of chimeric IgE/IgG and desensitization of cellular responses. Ph. D. thesis. Cornell University, Ithaca, NY. 241 pp.